THEORETICAL & APPLIED MECHANICS LETTERS **1**, 014001 (2011)

Study on hemodynamics in patient-specific thoracic aortic aneurysm

Ai-Ke Qiao,[1, a)] Wen-Yu Fu,[2,3] and You-Jun Liu[1, b)]
[1)] *College of Life Science and Bioengineering, Beijing University of Technology, Beijing 100124, China*
[2)] *College of Mechanical and Electrical Engineering, Beijing Union University, Beijing 100124, China*
[3)] *College of Mechanical Engineering and Applied Electronics Technology, Beijing University of Technology, Beijing 100101, China*

(Received 26 October 2010; accepted 23 November 2010; published online 10 January 2011)

Abstract The objective of this study is to investigate the hemodynamics in patient-specific thoracic aortic aneurysm and discuss the reason for formation of aortic plaque. A 3-Dimensional pulsatile blood flow in thoracic aorta with a fusiform aneurysm and 3 main branched vessels was studied numerically with the average Reynolds number of 1399 and the Womersley number of 19.2. Based on the clinical 2-Dimensional CT slice data, the patient-specific geometry model was constructed using medical image process software. Unsteady, incompressible, 3-Dimensional Navier-Stokes equations were employed to solve the flow field. The temporal distributions of hemodynamic variables during the cardiac cycle such as streamlines, wall shear stresses in the arteries and aneurysm were analyzed. Growth and rupture mechanisms of thoracic aortic aneurysm in the patient can be analyzed based on patient-specific model and hemodynamics simulation. © *2011 The Chinese Society of Theoretical and Applied Mechanics.* [doi:10.1063/2.1101401]

Keywords thoracic aneurysm, CT image, CFD model, wall shear stress, hemodynamics

Studies have shown that hemodynamic parameters such as wall shear stress (WSS) and its change with time, wall pressure and flow velocity have an important relationship with aneurismal growth and rupture. Therefore, hemodynamic analysis based on a patient-specific model should be performed and then applied to predict possibility of aneurismal rupture and make surgical planning. Characteristics of hemodynamic parameters are closely related to vascular geometry.[1–3] Numerical simulation of hemodynamics is an important research method in the biomechanical field where construction of an accurate and effective patient-specific model is a key point. Many researchers have performed numerical simulations of blood flow in human thoracic aorta. Numerical simulation of a patient-specific model for thoracoabdominal aortic aneurysm was done in Ref. [1]. However, numerical simulation based on an aorta model with the large branches is very rare. For more realistic simulation of patient-specific thoracic aneurysm blood flow, a real vascular model containing ascending aorta, aortic arch and descending thoracic aorta was constructed based on CT images in this paper. This model also contains the innominate artery, left common carotid artery and left subclavian artery. More importantly, there is a fusiform aneurysm in the descending thoracic aorta. The objective of this study is to investigate the hemodynamics in patient-specific thoracic aortic aneurysm and provide a theoretical basis for aneurismal growth and rupture.

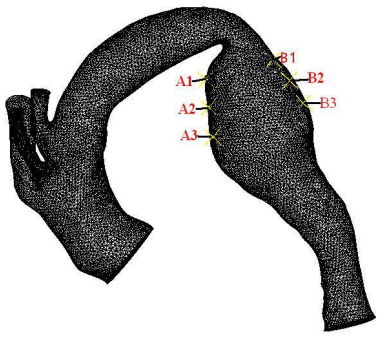

Fig. 1. 3-D model with surface mesh.

CT images of a female patient aged 75 years old were obtained from the Hospital of Tohoku University. A Toshiba Aquilion multi-slice spiral CT machine was used to scan the thoracic aorta. The original image file format was DICOM. The total number of scanning slices is 600 and the range of scanning is from neck to buttocks. The pixel size is 0.625 mm and resolution is 512×512. The distance between neighboring layers is 1 mm. The CT data was imported into Mimics software and data of the aortic vessel was extracted by means of 3-D threshold segmentation and 3-D region growing segmentation. An optimized model (Fig. 1) was then obtained in Mimics. Finally, a surface model of the thoracic aorta was exported in STL format which was then imported into ANSYS ICEM CFD 11.0. Volume meshes were generated by using mesh type of unstructural tetrahedron and prism. Progressively finer meshes were generated in the normal direction of the vessel wall so as to improve accuracy of calculation near the boundary layer. In order to reduce the dependence of calculation results on the grid size, many simulations with different volume mesh generation were repeated. When the relative error of WSS at the same location of previous and next mesh model is less than 4%, it is considered that independence of grid size has been reached. The initial boundary layer thickness was 0.05 mm, the number of layers was 5 and the thickness of every layer increased by a factor of 1.2 linearly. The total number of meshes was 4 100 000. The volume mesh file was imported into ANSYS CFX 11.0 to perform the numerical

[a)] Corresponding author. E-mail: qak@bjut.edu.cn
[b)] E-mail: lyjlma@bjut.edu.cn

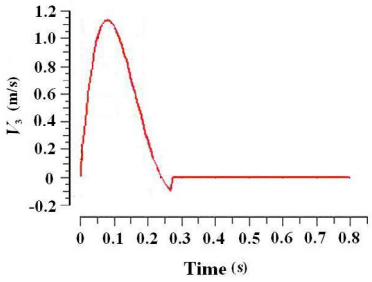

Fig. 2. Velocity at entrance in a cardiac cycle.

simulation.

The following assumptions were employed in this numerical study: non-permeability and rigid vascular wall; incompressible Newtonian fluid; pulsatile and laminar flow. Viscosity and density of blood are 0.003 5 Pa·s and 1050 kg/m^3 respectively. Heart rate is 75 beats/min, so periods of cardiac cycle is 0.8 s. Womersley number based on the thoracic aorta diameter is 19.2. The average value of Reynolds number based on the entrance flow velocity and the thoracic aorta diameter is 1399.

A profile of the input velocity is shown in Fig. 2.[4] No-slip condition was applied to the vascular wall. Each exit at the innominate artery, left common carotid artery and left subclavian artery was assigned a proportion of 5% of the inlet flow. An opening boundary condition with relative static pressure of 0 Pa was assumed at the exit of the descending aorta. Thediscrete form of differential equations with upwind scheme and second order accuracy was used. A separate time step independence test was carried out and transient calculations of time step of 0.01, 0.005 and 0.0025 s were performed. The same criterion to the independence of grid was used to determine the time step. After three calculations it was found that the time step of 0.005 is an appropriate value. The largest residual of root-mean-square was set to 10^{-5}, and the maximum number of iterations at each time step was set to 200. In this way precision of calculation was ensured. Convergence solutions were obtained after three cycles of iterative calculations. In order to reduce calculation time, parallel calculation was used.

Several typical moments were selected to show the calculation results of streamline, WSS and its change with time.

Streamlines at different moments in a cardiac cycle are shown in Fig. 3. As shown in Fig. 3, there were large vortexes in the descending aortic aneurysm cavity. This was the main difference of flow characteristics in the thoracic aorta with aneurysm and without aneurysm (refer to Ref. [5] for analysis of flow characteristics without aneurysm). In diastolic flow vortex characteristics were more apparent, and there were several vortices; especially in the latter half of the diastolic phase, there was a large vortex of blood flow in the descending aortic aneurysm. Therefore residence time of blood cells and other particles in the cavity of the aneurysm was increased, and the probability that these particles were

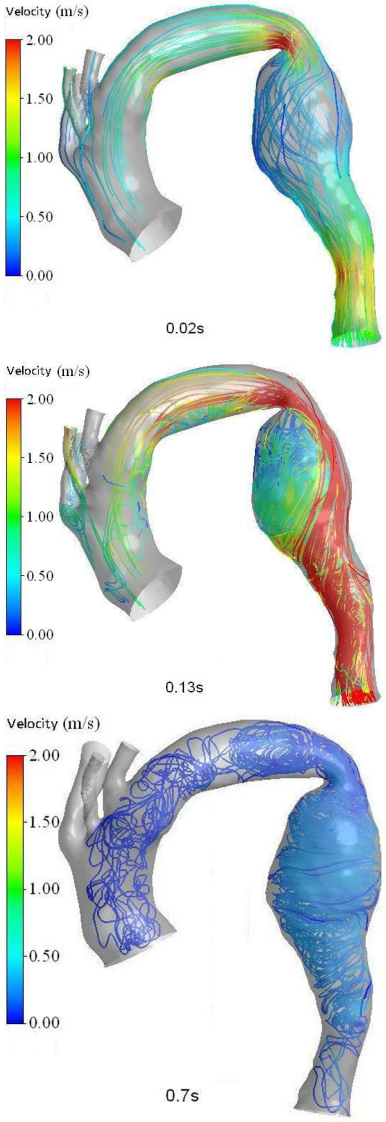

Fig. 3. Streamlines of blood flow in a cardiac circle.

deposited on these positions increased too. Those factors would increase the growth of aneurysm.[5]

WSS is related to aneurismal development and rupture. As shown in Fig. 4, the maximum WSS in systole appears in the neck of aneurysm. As shown in Fig. 5 (chart of WSS represents change at 6 points on the aneurismal wall in a cardiac circle), WSS changes over time (especially in the systole). WSSs on the aneurismal wall are significantly less than WSSs on other parts in accelerated phase of systole (0.02 s). In the decreasing phase of systolic (0.13 s), WSS at the outboard wall of the descending aortic aneurysm is significantly larger than that at the inboard wall. The value of WSS is also maintained at a relatively low range on the main part of the inboard wall. In the diastole (0.7 s), aneurismal WSS changes slightly, which can also be seen from Fig. 5. As shown in Fig. 4, the value of WSS at the inboard wall of descending aneurysm is small. Vortex flow always exists in this region throughout the car-

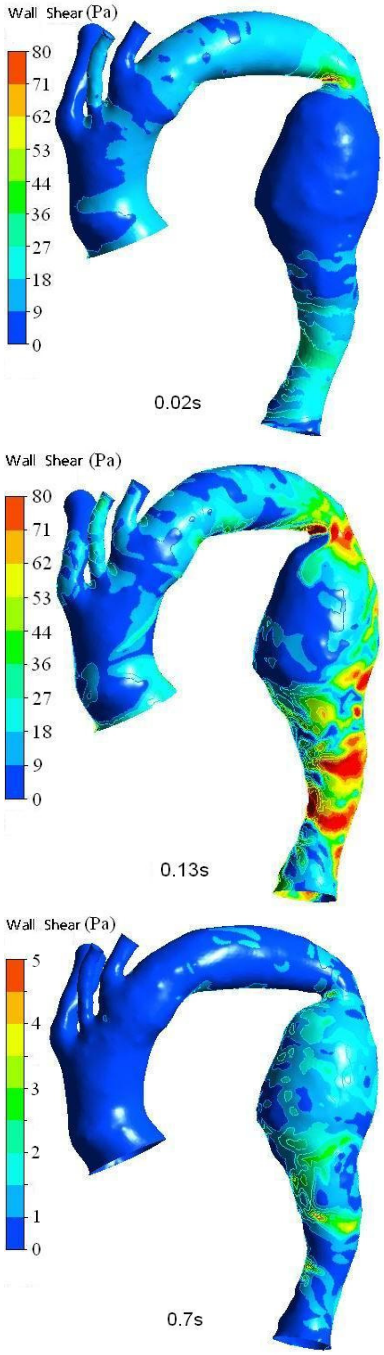

Fig. 4. Wall pressure distribution of blood flow in a cardiac.

diac cycle. Therefore, the residence time of a blood particle is longer in this region. Now it is widely recognized that low WSS and long residence time of particles are the most dangerous factors of hemodynamics in artery disease. Therefore, the inboard wall of a descending aneurysm may be the dangerous part where an aneurysm would continue to grow or even rupture. As far as clinical application, these results help us to spot critical areas where platelets or low-density lipoproteins may clump together. Finally, it helps us with design optimization of stent-grafts. A1, A2, A3 are located

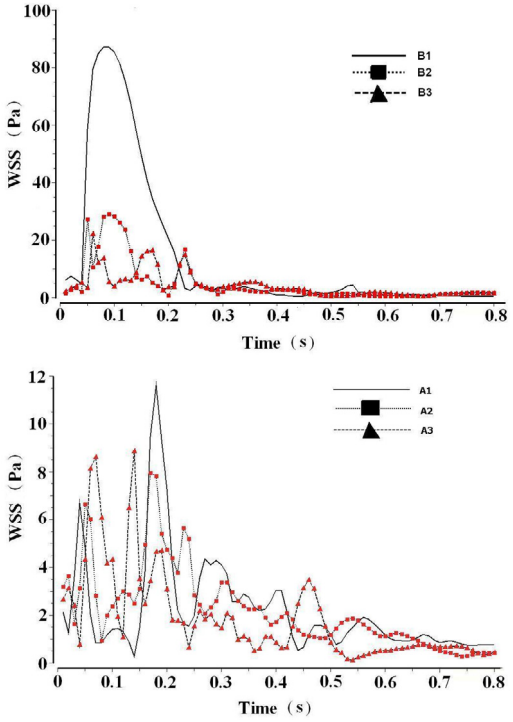

Fig. 5. Wall shear stress distribution of blood flow in a cardiac circle.

in the inboard wall of descending aortic aneurysm, and B1, B2, B3 are located in the lateral wall of descending aortic aneurysm. Whether in systolic phase or diastolic phase, values of WSS at the lateral wall are bigger than that at the inboard wall. It is more evident to watch TAWSS (Time Average Wall Shear Stress, TAWSS) in Table 1.

The aneurysm represented in this model had been formed and was in development and change. Therefore, the result of the calculation obtained from this model can not be used to infer hemodynamic reasons for the formation of an aneurysm. A big vortex exists at the inner wall of an aneurysm for most of the time of one period, speed of blood flow in this region is slow and the residence time of blood particles is longer in this region. As a result the probability is that blood particle deposits in this region are increased too. The cumulative effect of this kind of deposition may cause aneurysm to grow continuously.

Flow characteristics besides aneurysm are similar to Refs. [2, 6–8] (comparison in quality and in quantitative), which also proved the validity of simulation in this article. The results presented may further contribute to the understanding of aneurysm biomechanics and ultimately aneurysm rupture prediction.[9] Using a similar method the outcome of alternative treatment plans for cardiovascular disease, related to patient-specific hemodynamics, can be calculated and hence clinical surgeons can make a reasonable treatment plan.

Aortic plaque is likely to arise in vascular bifurcation and bending vessels. Because of the inclination of aortic plaque's formation, it is reasonable to believe that its formation and development may associate with flow

Table 1. Time average wall shear stress of aneurismal wall.

Point	A1	A2	A3	B1	B2	B3
TAWSS (Pa)	13.8849	4.8673	4.1178	2.2154	2.2282	1.8519

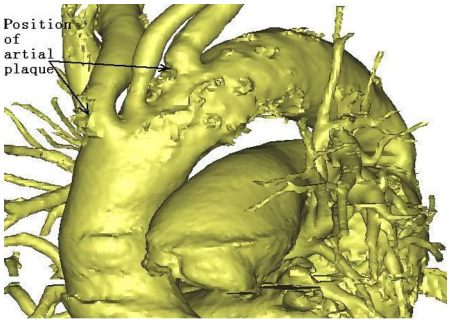

Fig. 6. Surface model without smooth process.

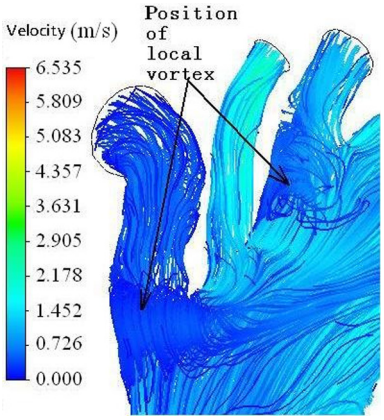

Fig. 7. Streamline of branched vessel.

characteristics in arteries and the geometrical shape of vessels. Particularly, that hemodynamic characteristics of local vessels at a special position and shape are closely related to the formation and development of aortic plaque.

The shape of a vessel that has formed aortic plaque is different from that has no aortic plaque. The different shape of the vessel must make flow characteristics different, especially local flow field characteristics. To explore hemodynamic factors resulting in aortic plaque, the characteristics of blood flow before aortic plaque is formed should be investigated. Then lookup whether there is a correlation between the actual location of aortic plaque and special flow features. The patient-specific model used in this study was acquired from a patient who suffered from aortic plaques at several positions. To study the relationship between blood flow features and the formation of aortic plaque, aortic plaque was removed during the process of creating the model.

The original 3-D surface model is shown in Fig. 6. A contrast agent was injected into arterial blood before the CT scan, so the CT attenuation value of arterial blood and arterial plaque is significantly different. After the CT images segmentation process, whose purpose was to extract the arterial vessel, the large artery plaques were removed. This is evident in Fig. 6 as is indicated by arrows. In order to study the relationship between the formation of arterial plaque and hemodynamic factors, these concave spaces were filled in the subsequent image processing.

In comparison between Fig. 6 and Fig. 7, it can be found that evident local vortex flows exist at positions where arterial plaques appear. Blood particles will stay longer in these regions because of the existence of the vortices. This will increase the probability that endothelial cells absorb mononuclear glomus cells and thus the probability of forming arterial plaque increases too.

With the construction and simulation of a patient-specific model of the thoracic aorta, distribution and changes of streamline and WSS in blood flow field were obtained. The hemodynamic reasons for the formation of arterial plaques were discussed preliminarily. This kind of model can be used for the calculation of thoracic aortic aneurysm hemodynamics and analysis of rupture mechanism of clinical thoracic aortic aneurysm in patients.

We would like to thank Dr. Makoto Ohta of Institute of Fluid Science in Tohoku University for providing us with the patient CT data. The work was supported by the National Natural Science Foundation of China (Grant Nos. 10972016 and 10872013) and Natural Science Foundation of Beijing (Grant Nos. 3092004 and 3092005).

1. A. Borghia, N. B. Wooda, R. H. Mohiaddinb, and X. Y. Xu, J. Fluids and Structures **24**, 270 (2008).
2. Y. Cai, S. X. Xu, Z. P. Jing, Z. Y. Mei, M. M. Liao, Q. S. Lu, and L. X. Yuan, J. Medical Biomechanics **23**, 140 (2008).
3. Y. M. Hoi, S. H. Woodward, M. Kim, D. B. Taulbee, and H. Meng, J. Biomechanical Engineering **128**, 843 (2006).
4. Z. H. Kang, *Cardiovascular Hemodynamics*, (Sichuan Education Press, Chengdu, China, 1990) 441 (in Chinese)
5. A. S. Mulay, *Computational Modeling of Cerebral Aneurysm Hemodynamic: Effect of Stenting*, Ph. D. thesis, State University of New York at Buffalo: 7 (2002).
6. Y. H. Lin, Z. P. Jing, Z. Q. Zhao, Z. J. Mei, X. Feng, R. Feng, and Q. S. Lu, Acad. J. Sec. Mil. Med. Univ. **27**, 867 (2006).
7. M. Markl, M. T. Draney, M. D. Hope, J. M. Levin, C. F. P. Han, and N. J. Alley, J. Computer Assisted Tomography **28**, 459 (2004).
8. H. G. Bogren and M. H. Buonocore, J. Magnetic Resonance Imaging **10**, 861 (1999).
9. B. J. Doyle, A. J. Cloonan, M. T. Walsh, D. A. Vorp, and T. M. McGloughlin, J. Biomechanics **43**, 1408 (2010).